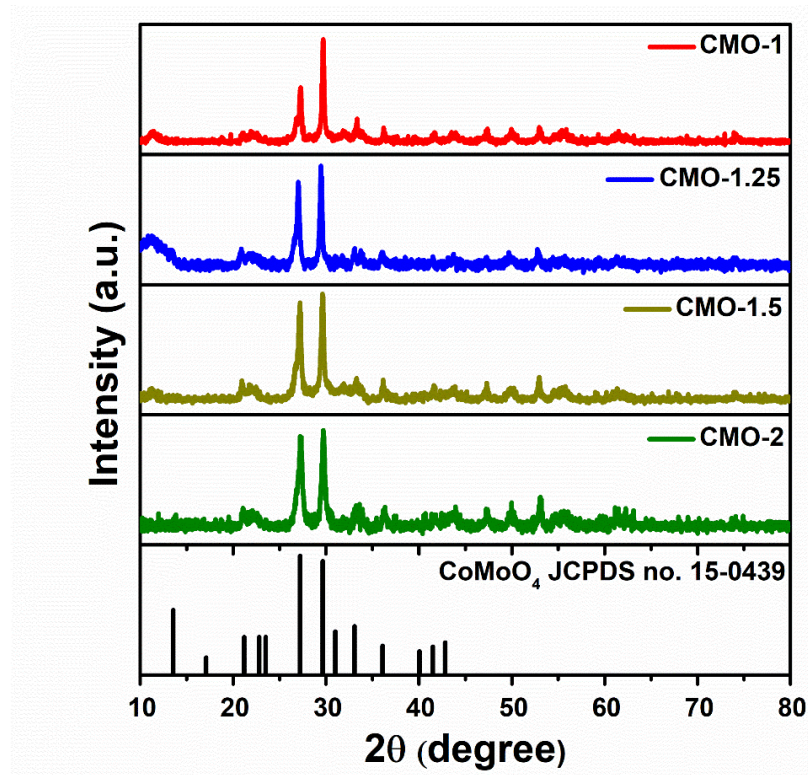


## Supplementary Information

### Heterointerface Engineering of Cobalt Molybdenum Suboxide for Overall Water Splitting

Renjith Nadarajan, Anju V. Gopinathan, Dileep N. Purayil, Akshaya S. Sidharthan, Manikoth M. Shajumon

School of Physics, Indian Institute of Science Education and Research Thiruvananthapuram, Maruthamala PO, Thiruvananthapuram, Kerala 695551, India.



**Fig. S1** XRD spectra of as-prepared CMO catalysts before annealing.

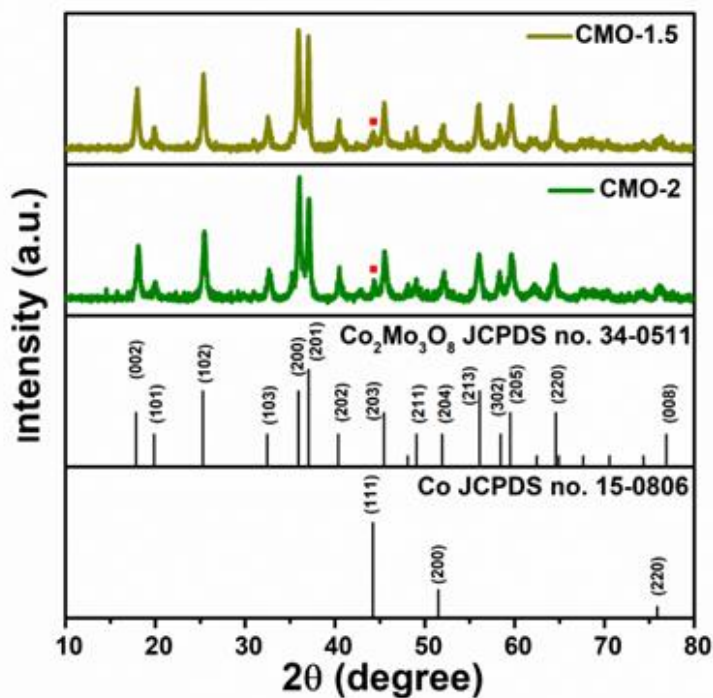


**Fig. S2** XRD spectra of CMO-1.5 and CMO-2 catalysts after annealing (■ corresponds to the (111) plane of Co).

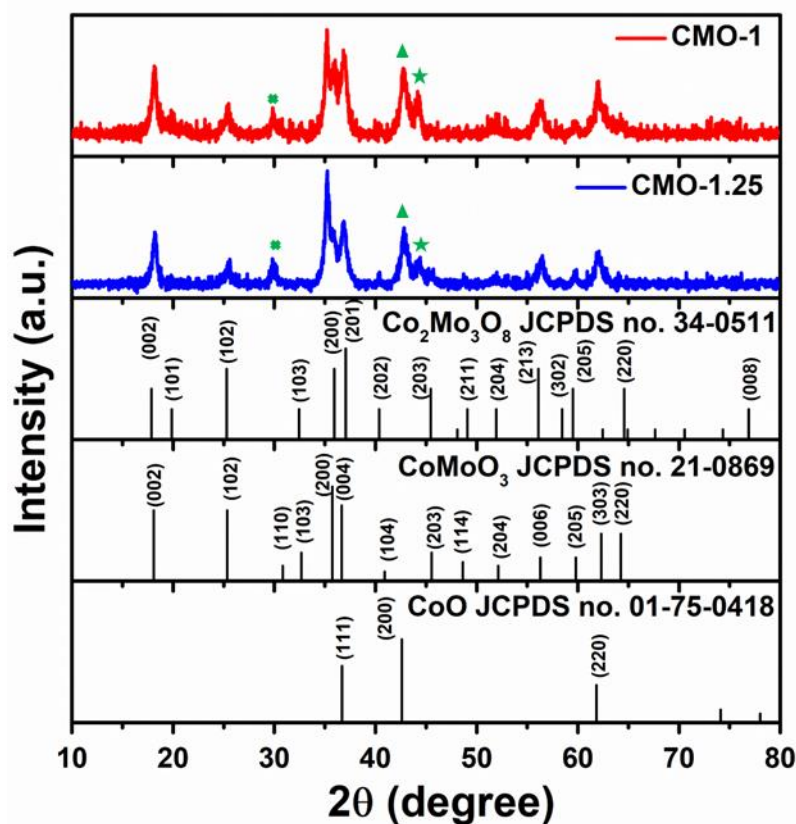


**Fig. S3** XRD spectra of CMO-1 and CMO-1.25 catalysts after annealing (★ corresponds to the (111) plane of Co & ▲ corresponds to (200) plane of CoO).

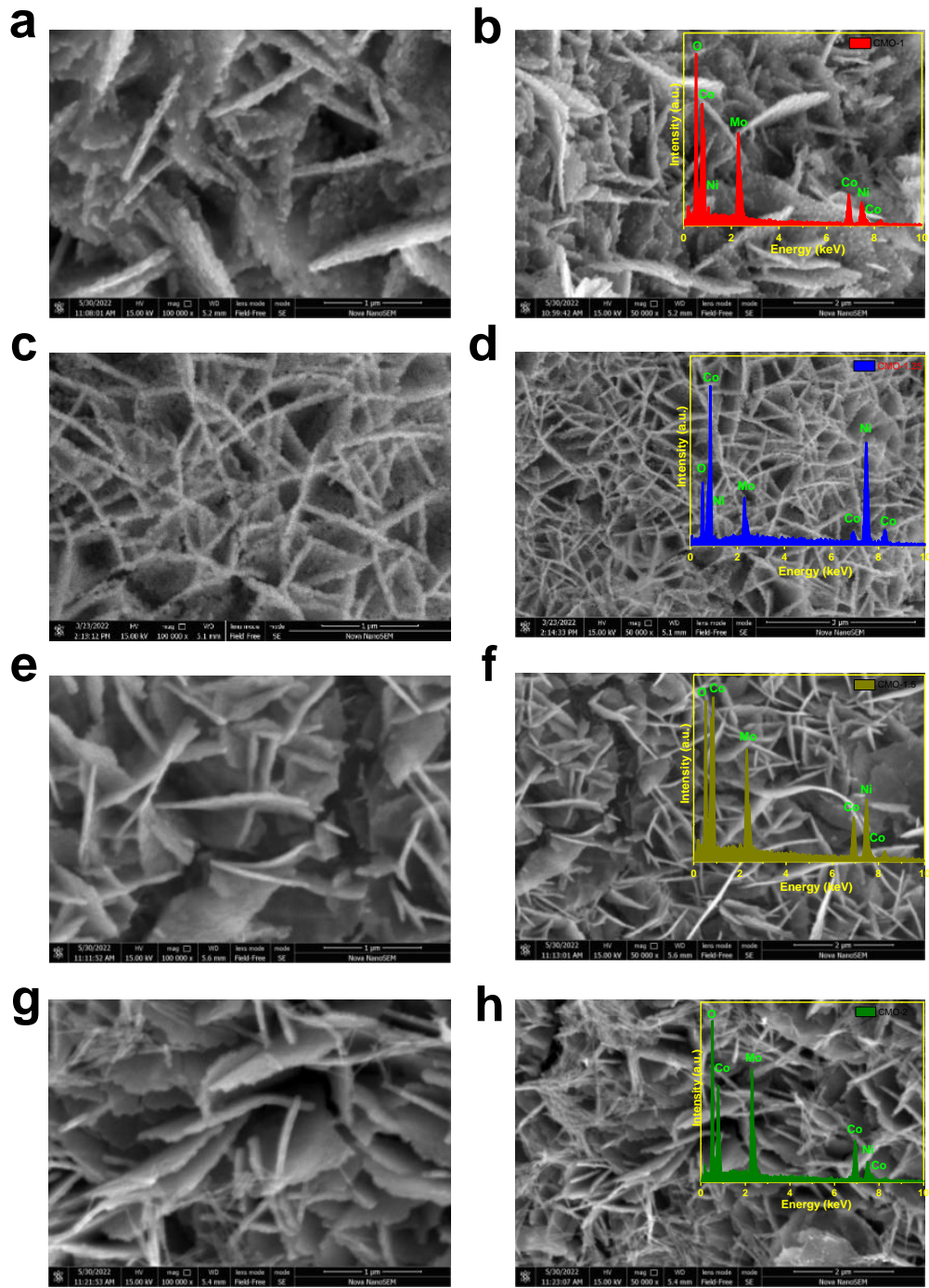


**Fig. S4.** SEM images of (a, b) CMO-1 (c, d) CMO-1.25 (e, f) CMO-1.5 and (g, h) CMO-2 catalysts. Inset showing the EDX spectrum collected from the respective catalysts.

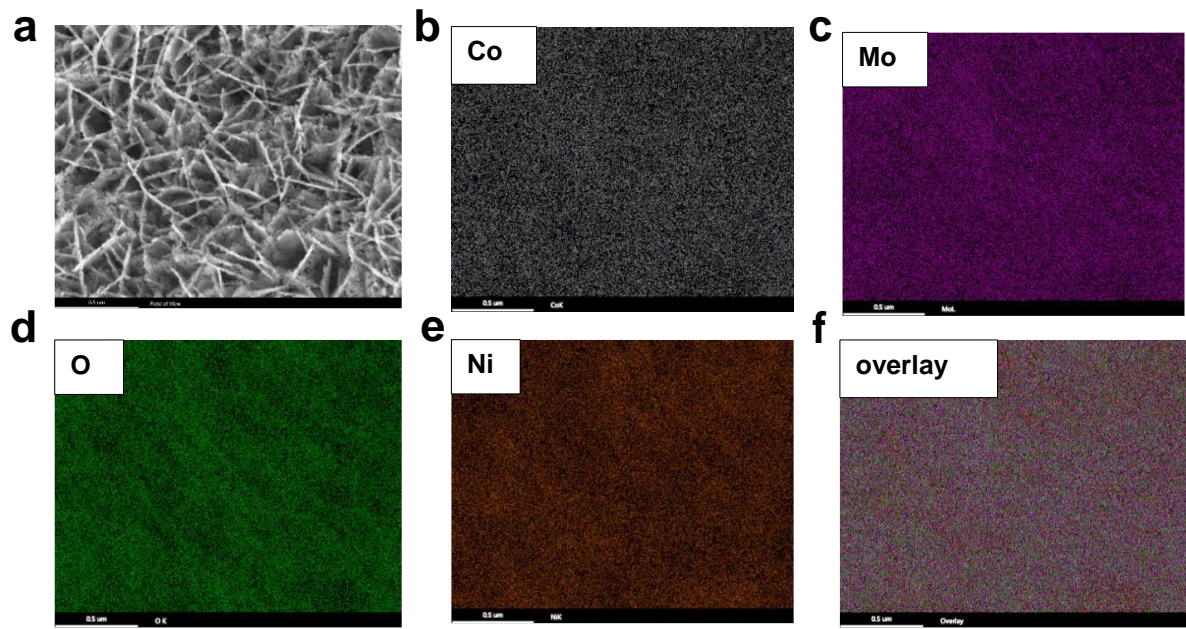


**Fig. S5** (a) SEM image of CMO-1.25 where EDX map was collected. EDX map of (b) Co (c) Mo (d) O (e) Ni and (f) overlay.

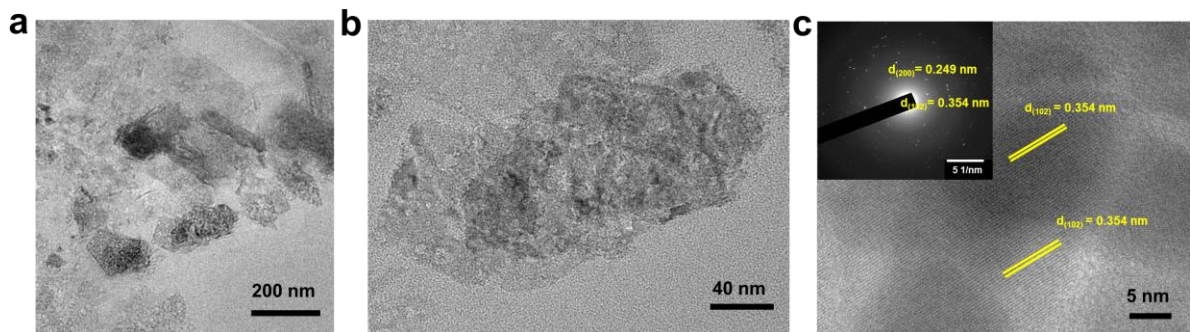


**Fig. S6.** (a, b) TEM images of CMO-2 (c) HR-TEM image of CMO-2, showing  $d$  spacing corresponding to  $\text{Co}_2\text{Mo}_3\text{O}_8$  (inset showing the SAED pattern).

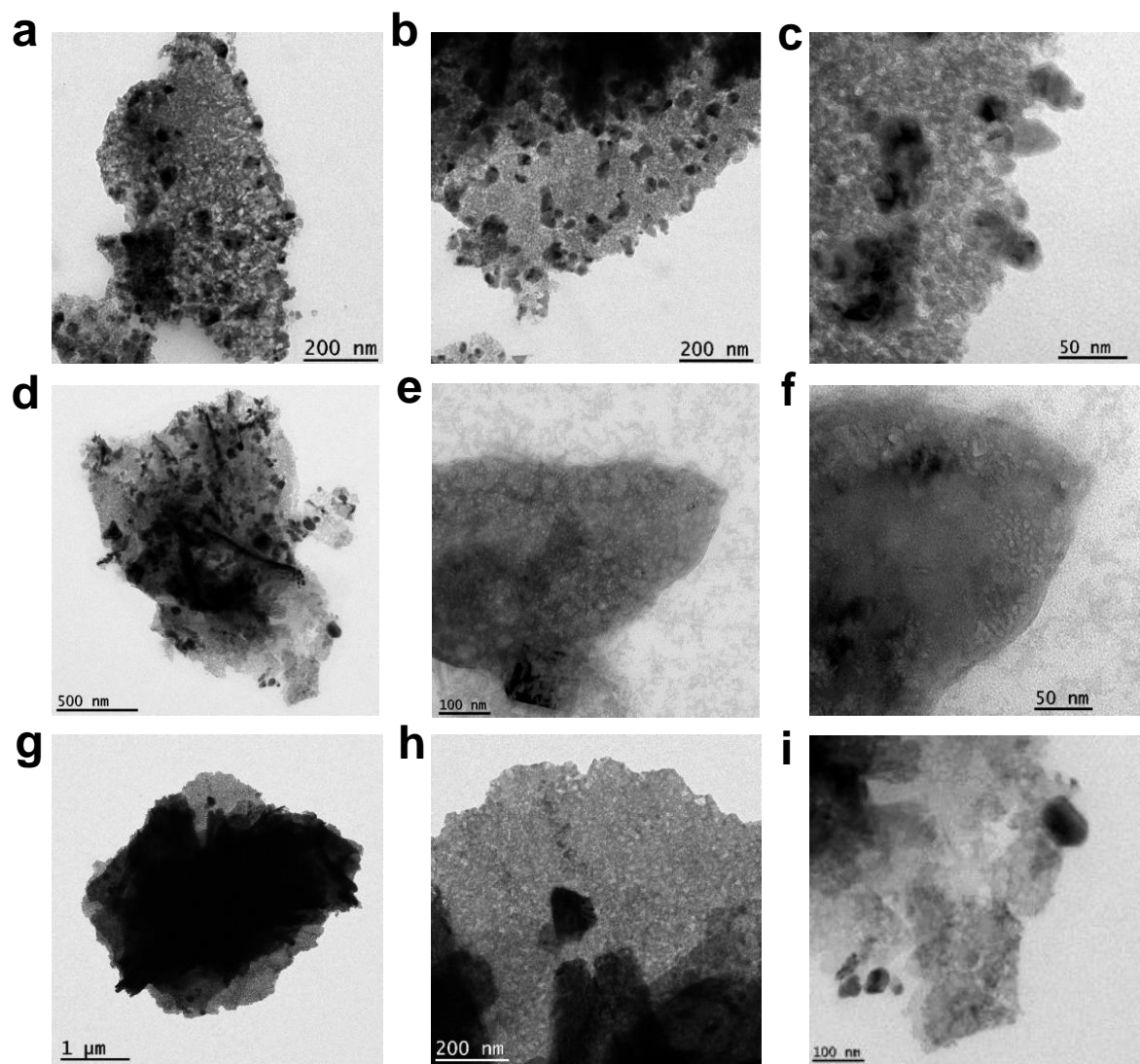


**Fig. S7.** TEM images of (a-c) CMO-1, (d-f) CMO-1.25 and (g-i) CMO-2.

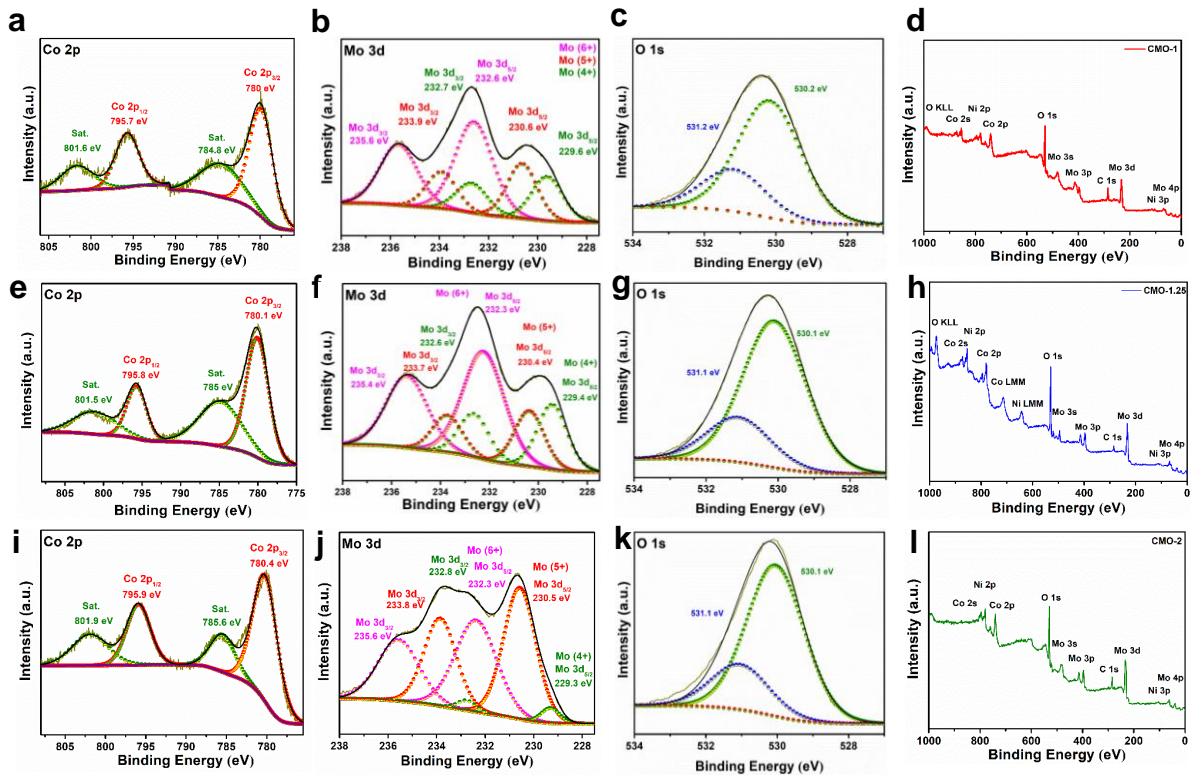


**Fig. S8.** XPS spectra (a) Co 2p, (b) Mo 3d, (c) O 1s and (d) survey spectrum of CMO-1 (e) Co 2p, (f) Mo 3d, (g) O 1s and (h) survey spectrum of CMO-1.25 (i) Co 2p, (j) Mo 3d, (k) O 1s and (l) survey spectrum of CMO-2.

**Table S1** XPS peak position and quantification of the percentage of different Mo species.

Sample	Co(2+)	Co(sat.)	Mo(4+)	Mo(5+)	Mo(6+)	% of Mo(6+)	% of Mo(5+)	% of Mo(4+)
CMO-1	780	784.8	229.6	230.6	232.6	53.0 %	25.6 %	21.4 %
	795.7	801.6	232.7	233.9	235.6			
CMO-1.25	780.1	785	229.4	230.4	232.3	55.3 %	20.6 %	24.1 %
	795.8	801.5	232.6	233.7	235.4			
CMO-2	780.4	785.6	229.3	230.5	232.3	45.5 %	51.1 %	3.4 %
	795.9	801.9	232.8	233.8	235.6			
CMO-1.25 after HER	780	784.7	229.0	230.1	232.0	47.8 %	41.4 %	10.8 %
	795.8	802.3	232.4	233.4	235.1			
CMO-1.25 after OER	780.8	784.8	229.6	230.8	232.4	29.7 %	66.7 %	3.6 %
	796.2	803.6	232.9	234.0	235.7			

**Table S2** ICP-OES data of different CMO catalysts.

Sample code	Element symbol and Wavelength (nm)	Concn. in ppm $\mu\text{g/ml}$ (or) mg/L	Molar concentration (mmol)	Co/Mo
CMO-1	Co 228.616	24.46	0.41	<b>0.97</b>
	Mo 202.031	40.94	0.42	
CMO-1.25	Co 228.616	27.77	0.47	<b>1.24</b>
	Mo 202.031	36.19	0.37	
CMO-1.5	Co 228.616	135.2	2.29	<b>1.65</b>
	Mo 202.031	133.7	1.39	
CMO-2	Co 228.616	90.93	1.54	<b>1.8</b>
	Mo 202.031	82.72	0.86	

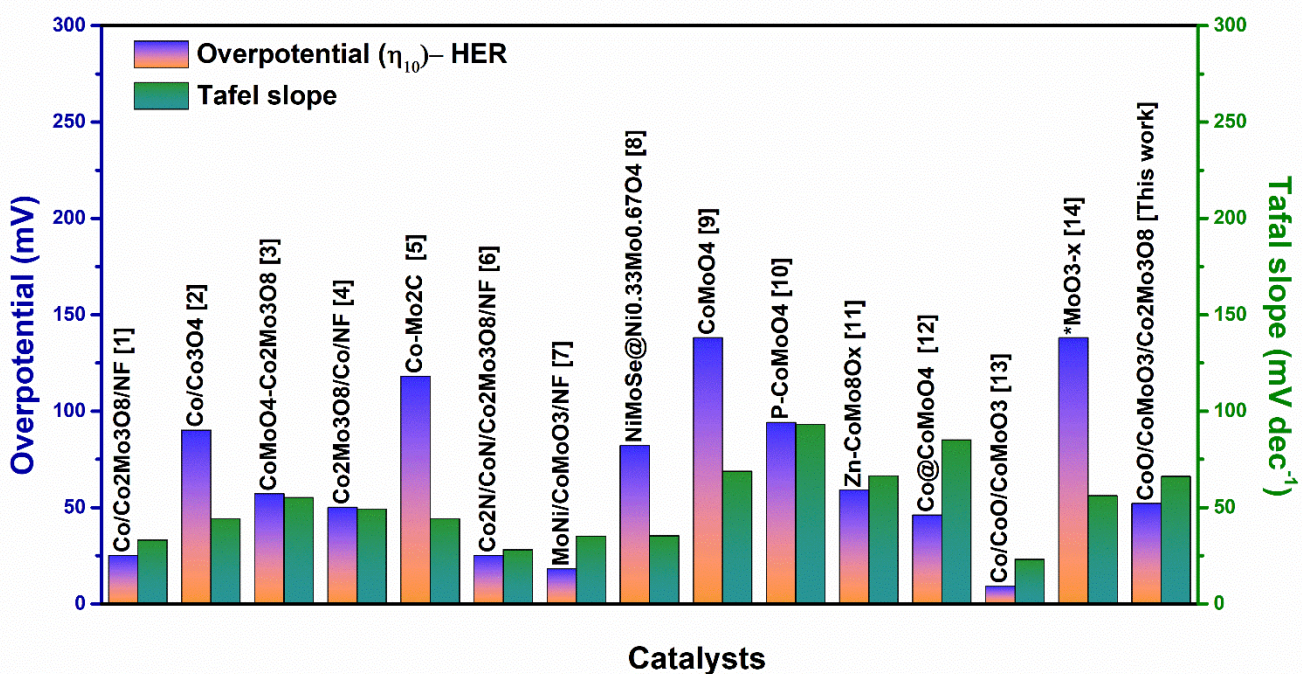


**Fig. S9.** Comparison of HER catalytic activities of different Co or Mo based non-noble metal electrocatalysts in alkaline solutions (\* represents in 0.1 M KOH).

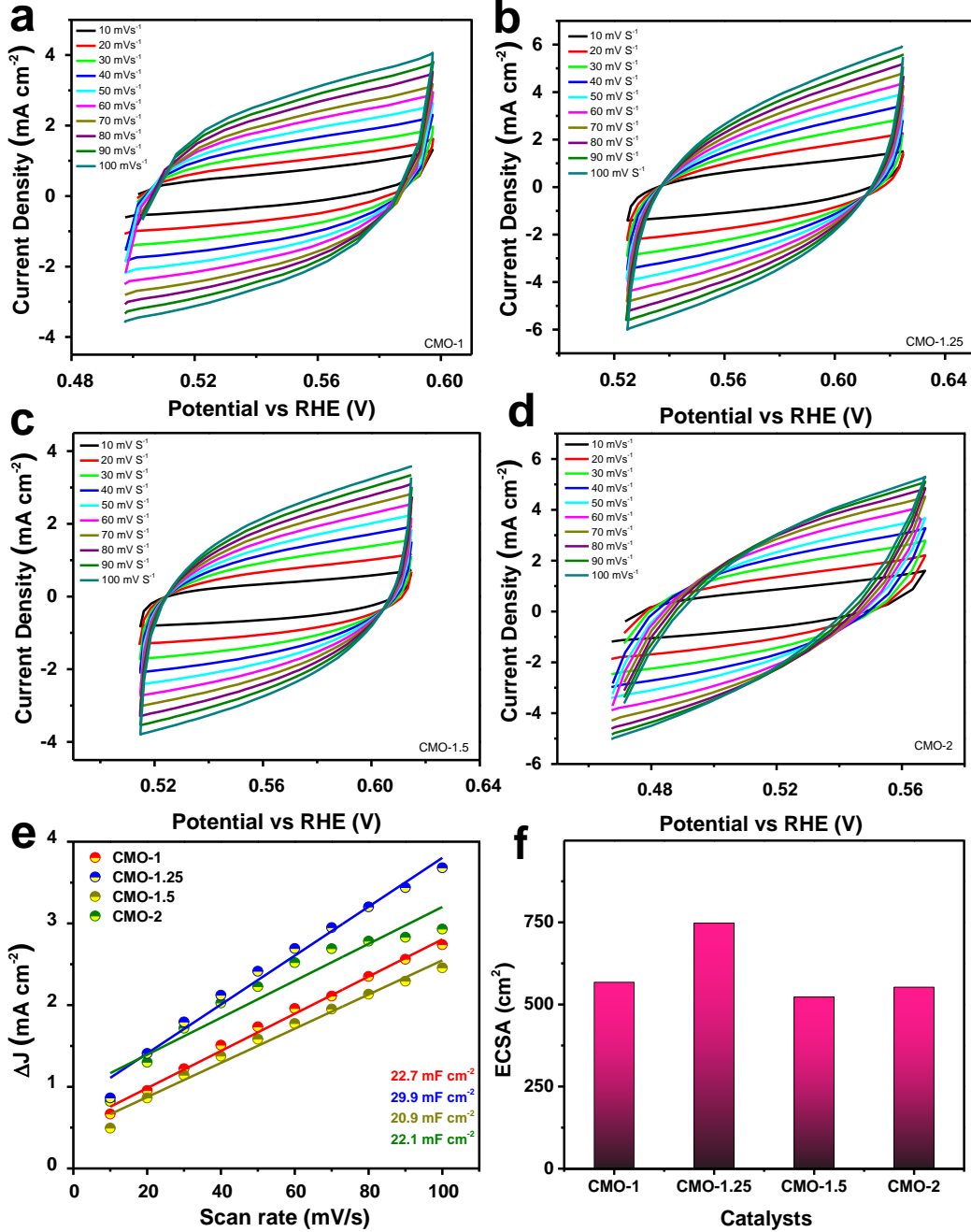


**Fig. S10.** Calculation of electrochemical double layer capacitance ( $C_{\text{dl}}$ ) of HER catalysts by plotting the current density variation for CMO based catalysts against the scan rates of cyclic voltammetry (CV) tests. Cyclic voltammetry tests at different scan rates in non-Faradaic regions for (a) CMO-1, (b) CMO-1.25, (c) CMO-1.5, (d) CMO-2 and (e) capacitive current densities at onset potentials as a function of scan rate. Here  $\Delta J$  is equal to  $\Delta J = \frac{J_a - J_c}{2}$  Where  $J_a$  and  $J_c$  are the anodic and cathodic current densities. The electrochemical double layer capacitance is obtained from the slope of the fitted straight line. (f) calculated ECSA for CMO catalysts.

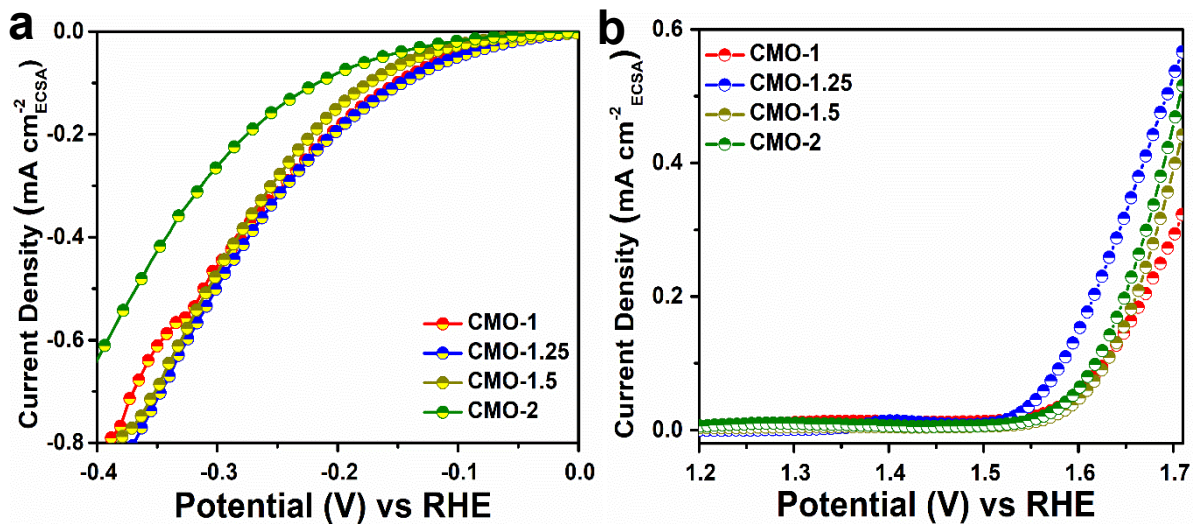


**Fig. S11** ECSA-normalized polarization curves of CMO catalysts for (a) HER and (b) OER.

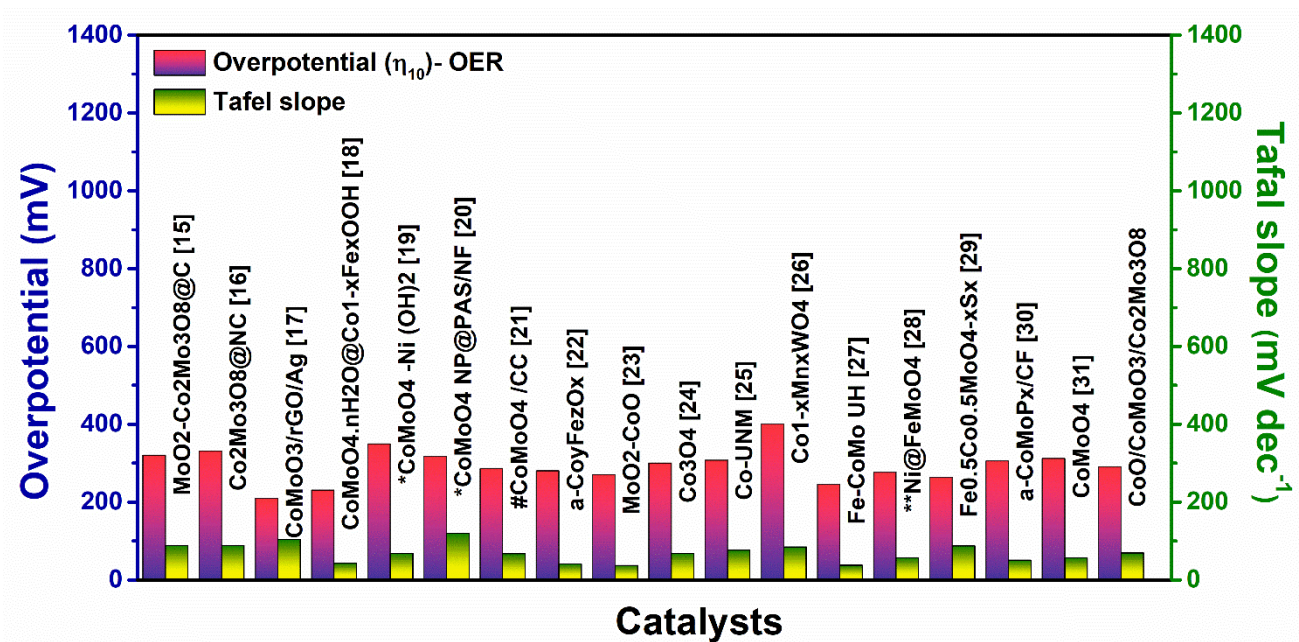


**Fig. S12.** The OER catalytic activities of different Co or Mo based non-noble metal electrocatalysts in alkaline solutions (\* represents overpotential for 100 mA cm<sup>-2</sup>, \*\* represents overpotential for 50 mA cm<sup>-2</sup> and # for overpotential for 15 mA cm<sup>-2</sup>).

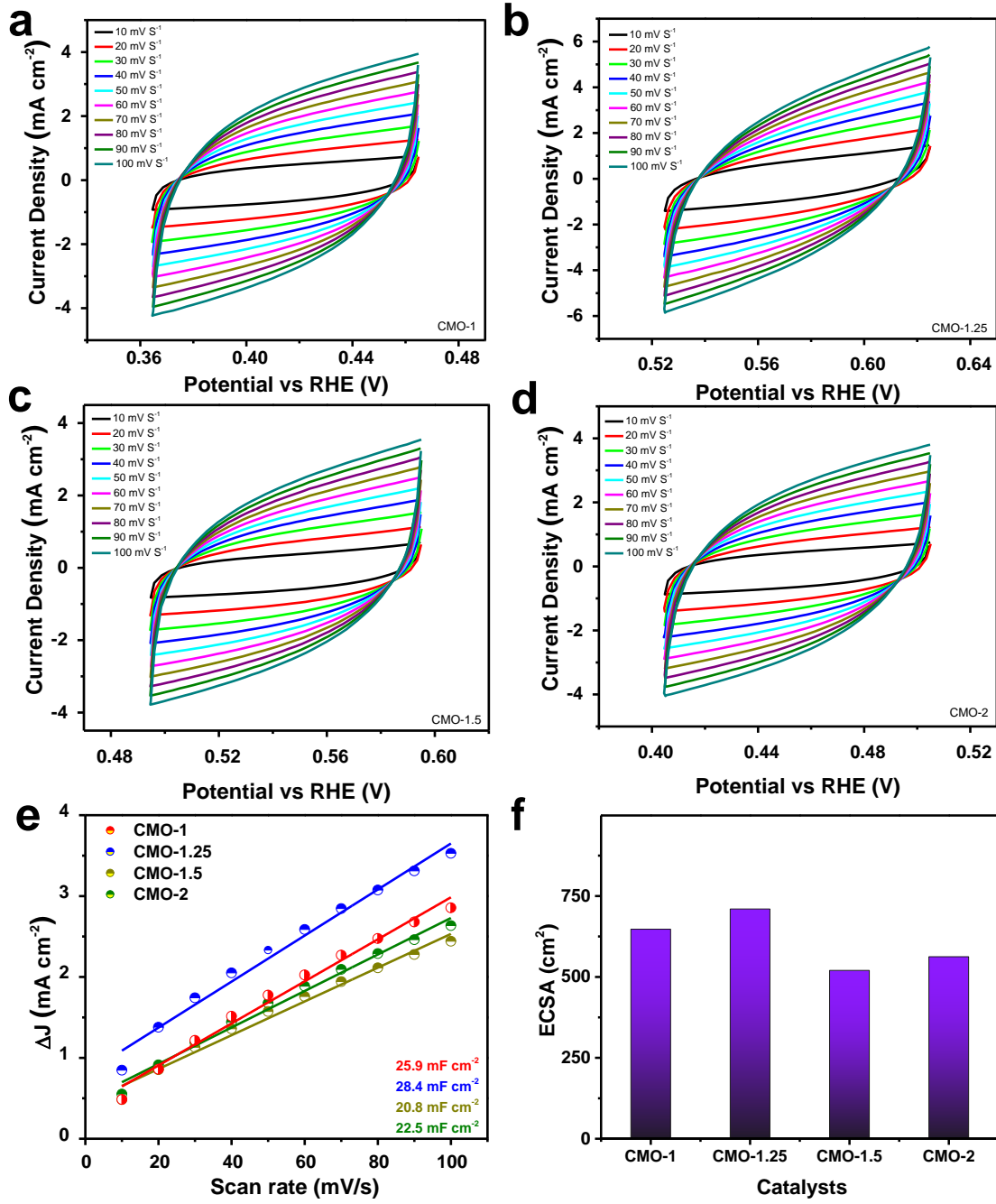


**Fig. S13.** Calculation of electrochemical double layer capacitance ( $C_{\text{dl}}$ ) of OER catalysts (a) Cyclic voltammetry (CV) tests at different scan rates in non-Faradaic regions for (a) CMO-1, (b) CMO-1.25, (c) CMO-1.5 and (d) CMO-2 (e) capacitive current densities at onset potentials as a function of scan rate. Here  $\Delta J$  is equal to  $\Delta J = \frac{J_a - J_c}{2}$  Where  $J_a$  and  $J_c$  are the anodic and cathodic current densities (f) calculated ECSA for CMO catalysts.

**Table S3** Comparison of the electrocatalytic activities of bifunctional electrocatalysts for overall water splitting.

Catalysts	HER $\eta_{10}$ value (mV)	HER Tafel slope $\text{mV dec}^{-1}$	OER $\eta_{10}$ value (mV)	OER Tafel slope $\text{mV dec}^{-1}$	Full cell potential for 10 mA cm $^{-2}$
<b>NiCo<sub>2</sub>O<sub>4</sub>@/CoMoO<sub>4</sub>/NF heterostructure [32]</b>	121	77	265 (20 mA cm $^{-2}$ )	102	1.55 V, 12 h
<b>NiCo<sub>2</sub>O<sub>4</sub> hollow micro cuboids [33]</b>	110	49.7	290	53	1.65 V, 36 h
<b>CoP [34]</b>	58	58.3	270 (50 mA cm $^{-2}$ )	116.4	1.66 (20 mA cm $^{-2}$ )
<b>NiS/Ni<sub>2</sub>P/CC heterostructures [35]</b>	111	78.1	265 (20 mA cm $^{-2}$ )	48.3	1.67 V, 10 h
<b>NiCo<sub>2</sub>S<sub>4</sub> nanowire arrays [36]</b>	263 (50 mA cm $^{-2}$ )	141	280 (20 mA cm $^{-2}$ )	89	1.68 V, 10 h
<b>Co<sub>7</sub>Fe<sub>3</sub> phosphide [37]</b>	166	88.9	225	37.9	1.56 V, 18 h
<b>Mo-Cu-Ni<sub>2</sub>P@NF [38]</b>	34	66	341 (100 mA cm $^{-2}$ )	79	1.50 V, 100 h
<b>Ni<sub>2</sub>P [39]</b>	96	94	255	57	1.47 V, 12 h
<b>Phosphorus-Doped Co<sub>3</sub>O<sub>4</sub> Nanowire [40]</b>	97	86	260 (20 mA cm $^{-2}$ )	60	1.63 V, 25 h
<b>CoS<sub>2</sub> nanotubes [41]</b>	193	88	276	81	1.67 V, 20 h

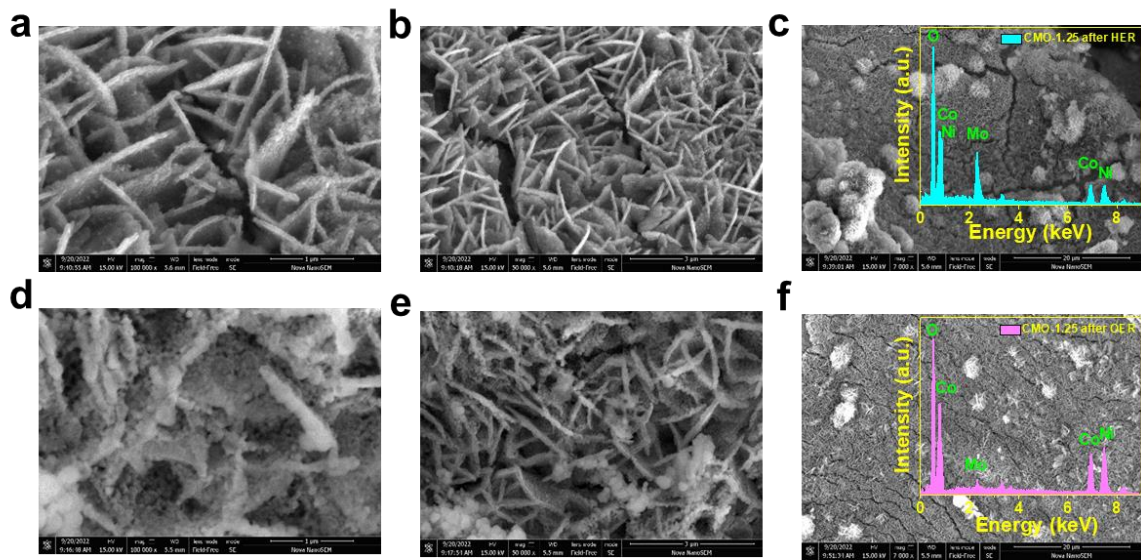


**Fig. S14.** SEM images of catalysts after 100 h stability tests (a-c) SEM images of CMO-1.25 after HER, inset showing the EDX spectra of sample (d-f) CMO-1.25 catalysts after OER, inset showing the EDX spectra of sample.

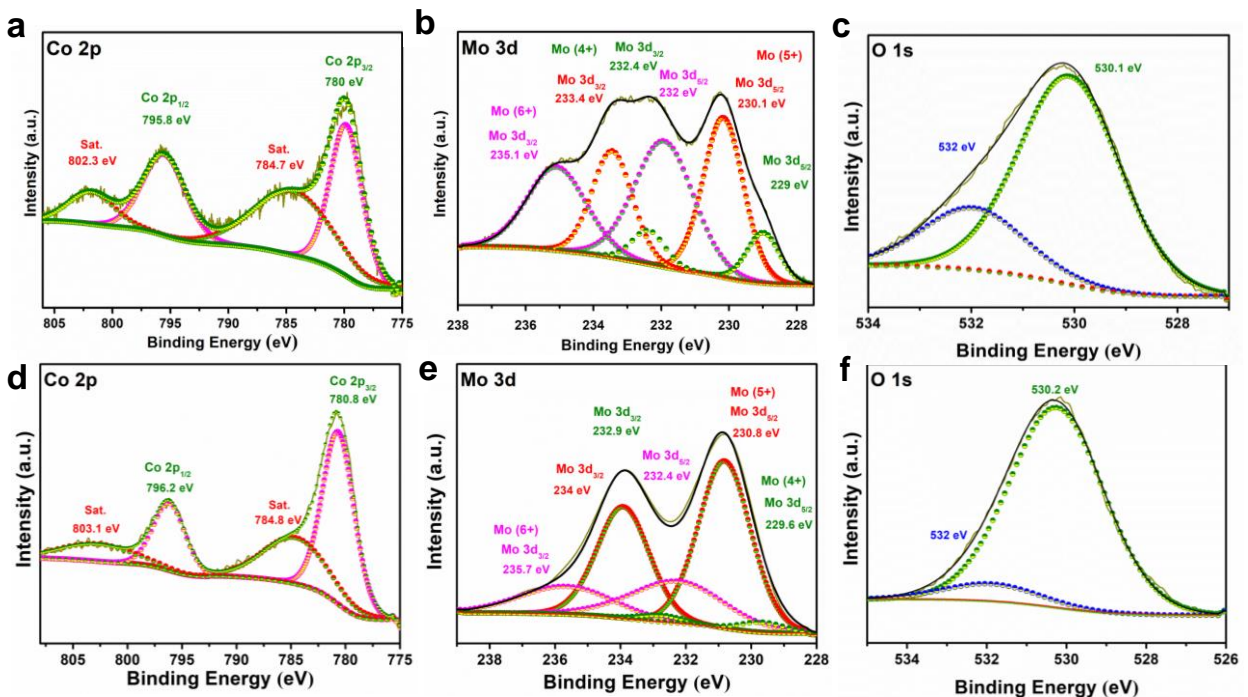


**Fig. S15.** XPS spectra (a) Co 2p, (b) Mo 3d and (c) O 1s of CMO-1.25 after HER (d) Co 2p, (e) Mo 3d and (f) O 1s of CMO-1.25 after OER.

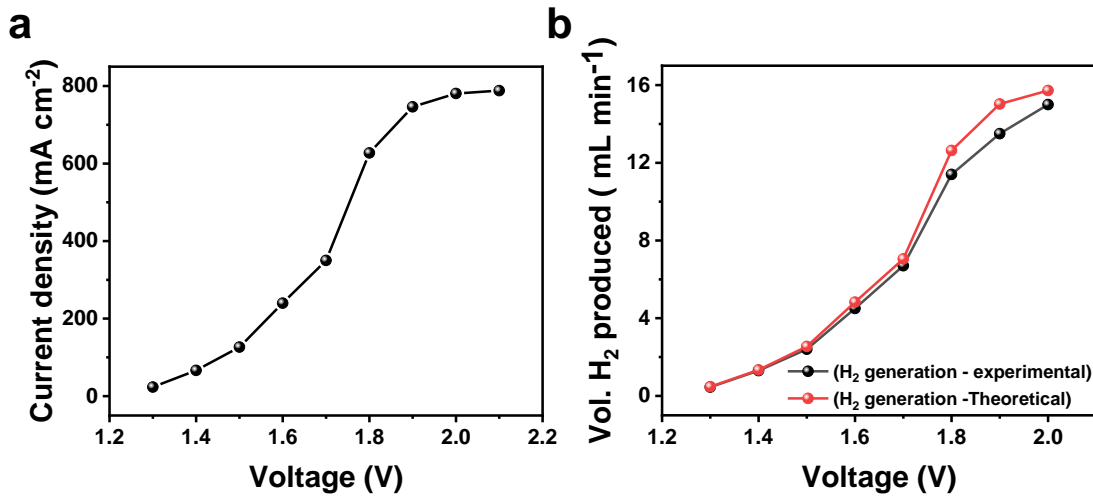


**Fig. S16.** (a) Potentiodynamic polarization curve for the water electrolyser assembled with CMO-1.25 catalyst as both anode and cathode (b) volume of hydrogen produced for the water electrolyser assembled with CMO-1.25 catalyst as both anode and cathode with different potentials.

The theoretical calculation for the volume of  $\text{H}_2$  production is as follows and is provided in the supplementary information.

*Volume of hydrogen (mL) evolved for a minute*

$$= (\text{Current}(A) \times \text{Time (sec)} \times 22400 \text{ (mL/mol)})/2F$$

Where F is Faraday's constant.

**Table S4** Comparison of the electrocatalytic activities of catalysts for overall water splitting in electrolyser setup.

Electrolyser design	Membrane used	Electrolyte	Temperature	Current density @ 1.8V ( $\text{mA cm}^{-2}$ )	References
CMO-1.25 <sup>(+)</sup>    CMO-1.25 <sup>(-)</sup>	FAS-50	1 M KOH	60°C	670 $\text{mA cm}^{-2}$	This work
NiFeV <sup>(+)</sup>   Co/CoO/CoMoO <sub>3</sub> <sup>(-)</sup>	FAA-3-PK-130	1 M KOH	--	100 $\text{mA cm}^{-2}$ @ 2.05 V	[13]
NiFe <sup>(+)</sup>    NiMo <sup>(-)</sup>	xQAPS	Pure water	70°C	400 $\text{mA cm}^{-2}$	[42]
NCT-2 <sup>(+)</sup>    NCT-2 <sup>(-)</sup>	Tokuyama (A201)	1 M KOH	--	170 $\text{mA cm}^{-2}$ @ 2.0V	[43]
NiCPs <sup>(+)</sup>    NiCPs <sup>(-)</sup>	Tokuyama (A201)	1M KOH	70°C	150 $\text{mA cm}^{-2}$ @ 1.9V	[44]
Li <sub>0.21</sub> Co <sub>2.79</sub> O <sub>4</sub> <sup>(+)</sup>    Li <sub>0.21</sub> Co <sub>2.79</sub> O <sub>4</sub> <sup>(+)</sup>	(QPDTB-OH <sup>-</sup> )	Deionised water	30°C	300 $\text{mA cm}^{-2}$ @ 2.05V	[45]
Steel mesh <sup>(+)</sup>    steel mesh	Zirfon (Agfa)	30% KOH	70°C	100 $\text{mA cm}^{-2}$ @ 1.83 V	[46]

## Reference

- 1 M. Zang, N. Xu, G. Cao, Z. Chen, J. Cui, L. Gan, H. Dai, X. Yang and P. Wang, *ACS Catal.*, 2018, **8**, 5062–5069.
- 2 X. Yan, L. Tian, M. He and X. Chen, *Nano Lett.*, 2015, **15**, 6015–6021.
- 3 Z. Liu, C. Zhan, L. Peng, Y. Cao, Y. Chen, S. Ding, C. Xiao, X. Lai, J. Li, S. Wei, J. Wang and J. Tu, *J. Mater. Chem. A*, 2019, **7**, 16761–16769.
- 4 Y. Ou, W. Tian, L. Liu, Y. Zhang and P. Xiao, *J. Mater. Chem. A*, 2018, **6**, 5217–5228.
- 5 H. Lin, N. Liu, Z. Shi, Y. Guo, Y. Tang and Q. Gao, *Adv. Funct. Mater.*, 2016, **26**, 5590–5598.
- 6 W. Hu, Q. Shi, Z. Chen, H. Yin, H. Zhong and P. Wang, *ACS Appl. Mater. Interfaces*, 2021, **13**, 8337–8343.
- 7 D. Wang, C. Han, Z. Xing, Q. Li and X. Yang, *J. Mater. Chem. A*, 2018, **6**, 15558–15563.
- 8 T. He, Y. He, H. Li, X. Yin, L. Zhou, H. Shi, J. Ma and L. Chen, *J. Electroanal. Chem.*, 2022, **904**, 115829.
- 9 S. Li, N. Yang, L. Liao, Y. Luo, S. Wang, F. Cao, W. Zhou, D. Huang and H. Chen, *ACS Appl. Mater. Interfaces*, 2018, **10**, 37038–37045.
- 10 S. Zhao, J. Berry-Gair, W. Li, G. Guan, M. Yang, J. Li, F. Lai, F. Corà, K. Holt, D. J. L. Brett, G. He and I. P. Parkin, *Adv. Sci.*, 2020, **7**, 1–9.
- 11 M. Wang, M. Zhang, W. Song, L. Zhou, X. Wang and Y. Tang, *Inorg. Chem.*, 2022, **61**, 5033–5039.
- 12 R. Xiang, Y. Duan, L. Peng, Y. Wang, C. Tong, L. Zhang and Z. Wei, *Appl. Catal. B Environ.*, 2019, **246**, 41–49.
- 13 B. Lin, J. Chen, R. Yang, S. Mao, M. Qin and Y. Wang, *Appl. Catal. B Environ.*, 2022, **316**, 121666.
- 14 Z. Luo, R. Miao, T. D. Huan, I. M. Mosa, A. S. Poyraz, W. Zhong, J. E. Cloud, D. A. Kriz, S. Thanneeru, J. He, Y. Zhang, R. Ramprasad and S. L. Suib, *Adv. Energy Mater.*, 2016, **6**, 1600528.
- 15 Y. Li, H. Xu, H. Huang, C. Wang, L. Gao and T. Ma, *Chem. Commun.*, 2018, **54**, 2739–2742.
- 16 T. Ouyang, X. T. Wang, X. Q. Mai, A. N. Chen, Z. Y. Tang and Z. Q. Liu, *Angew. Chemie - Int. Ed.*, 2020, **59**, 11948–11957.
- 17 B. Zhang, G. Liu, X. Yao, X. Li, B. Jin, L. Zhao, X. Lang, Y. Zhu and Q. Jiang, *ACS Appl. Nano Mater.*, 2021, **4**, 5383–5393.
- 18 J. Wang, H. Yin, Z. Chen, G. Cao, N. Xu, H. Wu and P. Wang, *Electrochim. Acta*, 2020, **345**, 1–8.

- 19 Y. Xu, L. Xie, D. Li, R. Yang, D. Jiang and M. Chen, *ACS Sustain. Chem. Eng.*, 2018, **6**, 16086–16095.
- 20 X. Guan, L. Yang, G. Zhu, H. Wen, J. Zhang, X. Sun, H. Feng, W. Tian, X. Chen and Y. Yao, *Sustain. Energy Fuels*, 2020, **4**, 1595–1599.
- 21 F. Wang, J. Zhao, W. Tian, Z. Hu, X. Lv, H. Zhang, H. Yue, Y. Zhang, J. Ji and W. Jiang, *RSC Adv.*, 2019, **9**, 1562–1569.
- 22 W. Zhang, G. Chen, Y. Du, S. Zhu, J. Zhang, G. Liu, F. Zhang, S. Wang and X. Wang, *ACS Appl. Energy Mater.*, 2022, **5**, 3129–3136.
- 23 B. B. Li, Y. Q. Liang, X. J. Yang, Z. D. Cui, S. Z. Qiao, S. L. Zhu, Z. Y. Li and K. Yin, *Nanoscale*, 2015, **7**, 16704–16714.
- 24 L. Xu, Q. Jiang, Z. Xiao, X. Li, J. Huo, S. Wang and L. Dai, *Angew. Chemie - Int. Ed.*, 2016, **55**, 5277–5281.
- 25 Y. Li, F. M. Li, X. Y. Meng, S. N. Li, J. H. Zeng and Y. Chen, *ACS Catal.*, 2018, **8**, 1913–1920.
- 26 G. Karkera, T. Sarkar, M. D. Bharadwaj and A. S. Prakash, *ChemCatChem*, 2017, **9**, 3681–3690.
- 27 L. Zeng, B. Cao, X. Wang, H. Liu, J. Shang, J. Lang, X. Cao and H. Gu, *Nanoscale*, 2021, **13**, 3153–3160.
- 28 J. J. Zhang, C. M. Yang, C. Q. Jin, W. W. Bao, R. H. Nan, L. Hu, G. Liu and N. N. Zhang, *Chem. Commun.*, 2021, **57**, 3563–3566.
- 29 B. Fei, Z. Chen, Y. Ha, R. Wang, H. Yang, H. Xu and R. Wu, *Chem. Eng. J.*, 2020, **394**, 124926.
- 30 H. Huang, A. Cho, S. Kim, H. Jun, A. Lee, J. W. Han and J. Lee, *Adv. Funct. Mater.*, 2020, **30**, 2003889.
- 31 M. Q. Yu, L. X. Jiang and H. G. Yang, *Chem. Commun.*, 2015, **51**, 14361–14364.
- 32 Y. Gong, Z. Yang, Y. Lin, J. Wang, H. Pan and Z. Xu, *J. Mater. Chem. A*, 2018, **6**, 16950–16958.
- 33 X. Gao, H. Zhang, Q. Li, X. Yu, Z. Hong, X. Zhang, C. Liang and Z. Lin, *Angew. Chemie - Int. Ed.*, 2016, **55**, 6290–6294.
- 34 Z. Duan, H. Liu, X. Tan, A. Umar and X. Wu, *Catal. Commun.*, 2022, **162**, 106379.
- 35 X. Xiao, D. Huang, Y. Fu, M. Wen, X. Jiang, X. Lv, M. Li, L. Gao, S. Liu, M. Wang, C. Zhao and Y. Shen, *ACS Appl. Mater. Interfaces*, 2018, **10**, 4689–4696.
- 36 D. Liu, Q. Lu, Y. Luo, X. Sun and A. M. Asiri, *Nanoscale*, 2015, **7**, 15122–15126.
- 37 Q. Chen, Q. Zhang, H. Liu, J. Liang, W. Peng, Y. Li, F. Zhang and X. Fan, *Small*, 2021, **17**, 1–8.
- 38 J. Li, Z. Zhang, X. Zhang, L. Xu, S. Yuan, H. Wei and H. Chu, *Dalt. Trans.*, 2021, **50**,

9690–9694.

- 39 N. Mushtaq, C. Qiao, H. Tabassum, M. Naveed, M. Tahir, Y. Zhu, M. Naeem, W. Younas and C. Cao, *Sustain. Energy Fuels*, 2020, **4**, 5294–5300.
- 40 Z. Wang, H. Liu, R. Ge, X. Ren, J. Ren, D. Yang, L. Zhang and X. Sun, *ACS Catal.*, 2018, **8**, 2236–2241.
- 41 C. Guan, X. Liu, A. M. Elshahawy, H. Zhang, H. Wu, S. J. Pennycook and J. Wang, *Nanoscale Horiz.*, 2017, **2**, 342–348.
- 42 L. Xiao, S. Zhang, J. Pan, C. Yang, M. He, L. Zhuang and J. Lu, *Energy Environ. Sci.*, 2012, **5**, 7869–7871.
- 43 P. Ganesan, A. Sivanantham and S. Shanmugam, *ACS Appl. Mater. Interfaces*, 2017, **9**, 12416–12426.
- 44 S. H. Ahn, B. S. Lee, I. Choi, S. J. Yoo, H. J. Kim, E. A. Cho, D. Henkensmeier, S. W. Nam, S. K. Kim and J. H. Jang, *Appl. Catal. B Environ.*, 2014, **154–155**, 197–205.
- 45 X. Wu and K. Scott, *Int. J. Hydrogen Energy*, 2013, **38**, 3123–3129.
- 46 B. Zayat, D. Mitra and S. R. Narayanan, *J. Electrochem. Soc.*, 2020, **167**, 114513.